Inorg. Chem. **2007**, *46*, 568–577

^{1}H NMR Direct Observation of Enantiomeric Exchange in Palladium(II) and Platinum(II) Complexes Containing *N*,*N*′ Bidentate Aryl-pyridin-2-ylmethyl-amine Ligands

Virginia Diez,[†] José V. Cuevas,*[,†] Gabriel García-Herbosa,[†] Gabriel Aullón,[‡] Jonathan P. H. Charmant,[§] Arancha Carbayo,[†] and Asunción Muñoz[†]

Departamento de Quínica, Universidad de Burgos, Plaza Misael Bañuelos S/N, 09001 Burgos, Spain, Departament de Química Inorgànica and Centre de Recerca en Química Teòrica, Universitat de Barcelona, Diagonal 647, 08028 Barcelona, Spain, and School of Chemistry, University of Bristol, Bristol BS8 1TS, U.K.

Received June 13, 2006

The complexes [$MCl_2(\kappa^2$-N∼N′)] (N∼N′ = 2-C_5H_4N–CH_2–NHAr; Ar = 4-MeC_6H_4, **a**; 2,6-$Me_2C_6H_3$, **b**; 4-$MeOC_6H_4$, **c**; 4-$CF_3C_6H_4$, **d**; M = Pd, **1a**–**d**; Pt, **2a**–**d**) have been prepared and fully stereochemically characterized both in the solid state and in solution. Their behavior in DMSO-d_6 solution is dependent on the substituents of the aryl group and on the metal. Complexes of palladium with substituents at the *para* position (**1a**, **1c**, **1d**) display a dynamic ^{1}H NMR pattern when the solutions are heated. An enantiomeric exchange $S\lambda/R\delta$ is suggested to explain such behavior. On the basis of the calculated negative $\Delta S^{\ddagger}$ values, an associative mechanism involving the solvent is proposed. Under the same conditions, analogous complexes of platinum (**2a**, **2c**, **2d**) proved to be unstable, and release of the N∼N′ ligand was observed. Complexes **1b** and **2b** show temperature-variable ^{1}H NMR spectra without any evidence accounting for enantiomeric exchange or decoordination. DFT calculations on models of **1a** and **1b** show that diastereomeric exchange $S\delta/S\lambda$ is a process where the complex with the higher sterical hindrance, **1b**, has a lower energy barrier.

Introduction

Coordination chemistry can provide new catalysts for enantioselective synthesis.[1] An interesting way to develop new catalysts is the coordination of chiral or prochiral ligands to the metal. In this regard, the stereoselective synthesis of transition metal complexes represents a significant challenge to coordination chemists,[2] and one successful approach has been the use of chiral ligands such as phosphines.[3−5] Alternatively, nitrogen stereocenters in amine ligands, which invert readily unless coordinated to a metal,[6] can be good candidates for this strategy. Recent examples of catalytic processes using the nitrogen atoms of prochiral amines are the reaction of *N*-acylimino esters with silyl enol ethers to afford the corresponding Mannich-type adducts,[7] or a Diels−Alder reaction.[8]

In our group, working with racemic mixtures of complexes (*R*,*S*)-[$PdCl_2$(N∼N′)] (N∼N′ = 2-C_5H_4N−CH_2−NH−Ar, having Ar as phenyl, *p*-tolyl, *p*-anisil), we have reported that deprotonation of these complexes affords binuclear complexes with bridging amido ligands.[9] Interestingly, the dimerization of the deprotonated complexes is diastereospecific affording racemic mixtures in which two *R*- or two *S*-monomers dimerize together (but no *R* with *S* "cross" dimerization has been observed). In addition to stereogenic

* To whom correspondence should be addressed. E-mail: jvcv@ubu.es.
† Universidad de Burgos.
‡ Universitat de Barcelona.
§ University of Bristol.

(1) Walsh, P. J.; Lurain, A. E.; Balsells, J. *Chem. Rev.* **2003**, *103*, 3297−3344.
(2) Knof, U.; von Zelewsky, A. *Angew. Chem., Int. Ed.* **1999**, *38*, 303−322.
(3) Johansson, M. J.; Kann, N. C. *Mini-Rev. Org. Chem.* **2004**, *1*, 233−247.
(4) Hoge, G. *J. Am. Chem. Soc.* **2004**, *126*, 9920−9921.
(5) Tang, W. J.; Zhang, X. M. *Angew. Chem., Int. Ed.* **2002**, *41*, 1612−1614.
(6) Buckingham, D. A.; Marzilli, L. G.; Sargeson, A. M. *J. Am. Chem. Soc.* **1969**, *91*, 5227−5232.
(7) Kobayashi, S.; Matsubara, R.; Nakamura, Y.; Kitagawa, H.; Sugiura, M. *J. Am. Chem. Soc.* **2003**, *125*, 2507−2515.
(8) Pelz, K. A.; White, P. S.; Gagne, M. R. *Organometallics* **2004**, *23*, 3210−3217.
(9) Cuevas, J. V.; Garcia-Herbosa, G.; Muñoz, A.; Garcia-Granda, S.; Miguel, D. *Organometallics* **1997**, *16*, 2220−2222.

10.1021/ic061060u CCC: $37.00
Published on Web 01/03/2007

Scheme 1

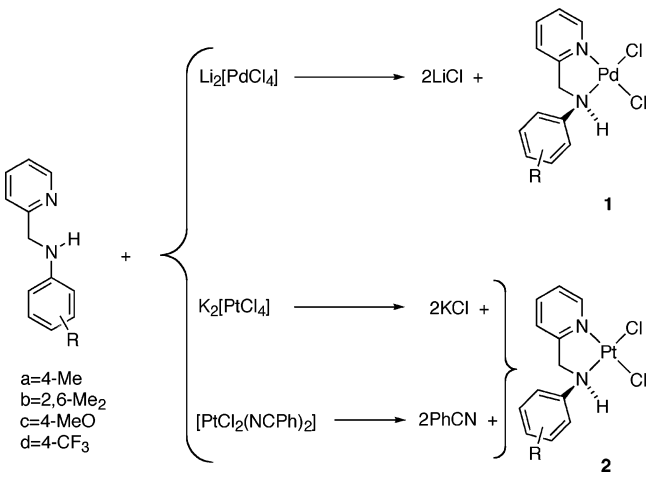

centers, other sources of chirality are the chirality associated with restricted rotations around some bonds in the backbone,[1] or the chirality associated with nonplanar chelating rings (δ/λ).[8,10−15]

In this work, we describe and explain the observed dynamic behavior of complexes $[MCl_2(\kappa^2\text{-N}\sim\text{N}')]$ (N∼N′ = 2-$C_5H_4N-CH_2-NHAr$; Ar = 4-MeC_6H_4, **a**; 2,6-$Me_2C_6H_3$, **b**; 4-$MeOC_6H_4$, **c**; 4-$CF_3C_6H_4$, **d**; M = Pd, **1a**−**d**; Pt, **2a**−**d**) in solution. DFT studies have proved to be valuable in explaining this dynamic behavior.

Results and Discussion

Syntheses of Compounds. Complexes $[MCl_2(\kappa^2\text{-N}\sim\text{N}')]$ (N∼N′ = 2-$C_5H_4N-CH_2-NHAr$; Ar = 4-MeC_6H_4, **a**; 2,6-$Me_2C_6H_3$, **b**; 4-$MeOC_6H_4$, **c**; 4-$CF_3C_6H_4$, **d**; M = Pd, **1a**−**d**; Pt, **2a**−**d**) were prepared by known methods (Scheme 1). The addition of methanolic solutions of ligands (**a**−**d**) to methanolic solutions of $Li_2[PdCl_4]$ afforded complexes **1a**−**d** as orange precipitates. The solids were collected and washed with diethyl ether. For the platinum complexes, addition of the ligand dissolved in water acidified with hydrochloric acid to a solution of $K_2[PtCl_4]$ in water yielded, after heating at reflux, complexes **2a**−**d** as yellow solids. The same products were obtained when a solution of the ligand in tetrahydrofuran was added to a solution of $[PtCl_2(NCPh)_2]$ in the same solvent and the mixture was heated at reflux for several hours.

Dynamic Behavior in Solution. The characterization of amine complexes **1** and **2** in solution was carried out in DMSO-d_6 because of their low solubility in other less polar solvents such as chloroform or acetone. In those complexes where the substituent of the aryl ring is in position 4 (i.e., ligands **a**, **c**, and **d**), the room temperature ^{1}H NMR spectra display a well resolved ABX spin system for the hydrogen atoms of the methylene group of the chelating ring (H^A and H^B) and the amine hydrogen atom (H^X).

Table 1. Chemical Shifts and Coupling Constants for the Methylenic Hydrogens[a]

compd	$\delta(H^A)$[b]	$\delta(H^B)$[b]	$\delta(H^A)-\delta(H^B)$[b]	$^2J(H^AH^B)$[c]	$^3J(H^AH^X)$[c]
1a	4.93	4.32	0.61	16.9	6.2
1c	4.90	4.30	0.60	16.8	5.4
1d	4.97	4.57	0.40	16.8	5.4
2a	4.75	4.41	0.34	16.9	6.2
2c	4.74	4.41	0.33	16.7	6.1
2d	4.84	4.63	0.21	16.9	6.1

[a] 400 MHz. ($^3J(H^BH^X)$ are close to 0 and not included). [b] Chemical shifts in ppm referenced to TMS. [c] Coupling constants in Hz and in absolute value.

Scheme 2

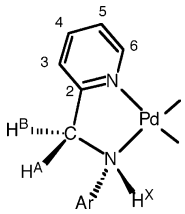

The signals corresponding to these diastereotopic AB nuclei are separated by about 0.5 ppm (see Table 1). Coupling constants between these two nuclei, J_{AB}, are in the range from 16.7 to 16.9 Hz. These two nuclei display different coupling constants to the H^X nucleus (the hydrogen atom bonded to the anilinic nitrogen atom). The stronger coupling, in the range 5.4−6.2 Hz, is to the downfield nucleus, H^A, while coupling constants are very close to 0 for the coupling to the upfield nucleus, H^B).

A NOESY experiment for complex **1a** displays NOE effects involving aromatic protons and the proton labeled as H^B (see Scheme 2). One effect is between proton H^B and the hydrogen localized in position 3 of the pyridyl ring, and the other is between proton H^B and protons in positions 2 and 6 (H^{ortho}) of the 1,4-disubstituted phenyl ring. However, the NOE effect between H^B and the aminic proton H^X is very weak. Furthermore, there is a clear NOE effect between H^A and H^X as shown in Figure 1.

On the other hand, when the substituents on the aryl group of the ligand are two methyl groups in the 2,6 positions (ligand **b**), the room temperature ^{1}H NMR spectra for complexes **1b** and **2b** display a smaller difference in the chemical shifts belonging to nuclei H^A and H^B, and the ^{1}H NMR spectra in the methylene region are quite different (see Figure 2).

At first glance, the spin system displayed for the methylenic hydrogens in complexes **1b** and **2b** could be interpreted as the result of dynamic behavior of the complex that makes equivalent both hydrogen atoms H^A and H^B on the time scale of the ^{1}H NMR experiment in spite of their diastereotopic character. On the contrary, the spin system of the same hydrogens in the other complexes could be reasonably interpreted as a nondynamic situation in which every hydrogen nucleus has its own chemical shift. The only

(10) Tudor, M. D.; Becker, J. J.; White, P. S.; Gagne, M. R. *Organometallics* **2000**, *19*, 4376−4384.
(11) Doherty, S.; Knight, J. G.; Hardacre, C.; Lou, H. K.; Newman, C. R.; Rath, R. K.; Campbell, S.; Nieuwenhuyzen, M. *Organometallics* **2004**, *23*, 6127−6133.
(12) Doherty, S.; Newman, C. R.; Rath, R. K.; van den Berg, J. A.; Hardacre, C.; Nieuwenhuyzen, M.; Knight, J. G. *Organometallics* **2004**, *23*, 1055−1064.
(13) Ashby, M. T.; Alguindigue, S. S.; Khan, M. A. *Organometallics* **2000**, *19*, 547−552.
(14) Ashby, M. T. *J. Am. Chem. Soc.* **1995**, *117*, 2000−2007.
(15) Ashby, M. T.; Govindan, G. N.; Grafton, A. K. *J. Am. Chem. Soc.* **1994**, *116*, 4801−4809.

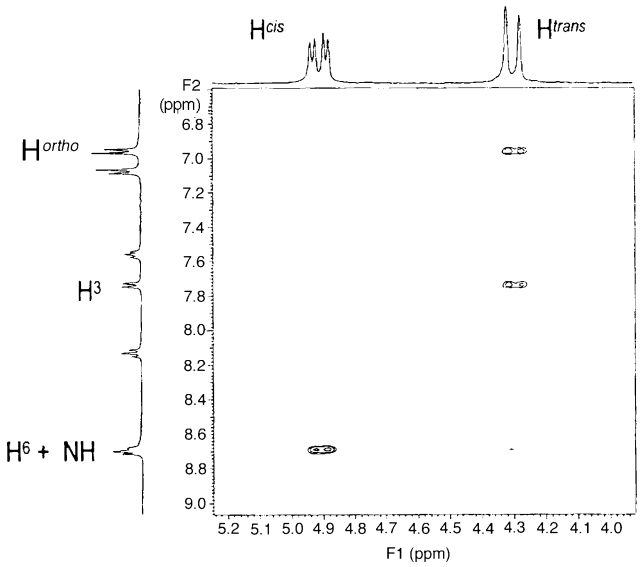

Figure 1. Expansion of the NOESY spectrum of **1a** showing the NOEs between proton H^B and aromatic protons, and NOEs between proton H^A and proton H^X.

apparent reason for such apparent dynamic behavior is the sterical hindrance of ligand **b**.

Variable Temperature Studies. These results encouraged us to record ^{1}H NMR spectra at variable temperature. As shown in Figure 3, heating a solution of **1d** in DMSO-d_6 causes the AB part of the ABX spin system to evolve into a broad two-signal system indicating the presence of a dynamic process. Complexes **1a** and **1c** (but not **1b**) behave similarly to **1d**. In view of this result, we conclude that in the palladium complexes with a *para* substituent in the aryl group (**1a**, **1c**, and **1d**) there is reversible dynamic behavior at temperatures above 303 K, in contrast to the static behavior observed in the room temperature ^{1}H NMR spectra.

This dynamic process can be related to conversion among the different structures arising from all the isomeric possibilities. In all these complexes there are two sources of chirality that lead to four different isomers. The coordinated amine nitrogen atom has four different substituents leading to a chiral center that can adopt *R* and *S* configurations. The other source of chirality is the nonplanar chelating ring adopting two conformations, δ and λ (Scheme 3).

The combination of these two sources of chirality gives rise to isomers $R\delta$, $S\delta$, $R\lambda$, and $S\lambda$. The isomers $R\delta$ and $S\lambda$ constitute an enantiomeric pair as do $S\delta$ and $R\lambda$. The relation between the pairs of enantiomers is that of diastereomers (i.e., $R\delta$, $S\lambda$ are diastereomers of $S\delta$, $R\lambda$).

In order to explain the dynamic behavior of the complexes in solution, two possibilities of isomerization can be considered. One possibility is $\delta-\lambda$ exchange of the chelating ring leaving the configuration of the nitrogen atom unchanged, for example, conformational exchange of $S\delta \leftrightarrows S\lambda$. This kind of dynamic behavior has already been described for other chelating rings.[16−19] The other possibility is inversion of configuration at the nitrogen atom, for example, $R\delta \leftrightarrows S\delta$. When considered separately, each isomerization process involves an interconversion between diastereomers, but if both processes occur simultaneously the overall interconversion is then between enantiomers.

Line-shape analysis of the variable temperature ^{1}H NMR spectra is consistent with both processes occurring simultaneously, that is, $R\delta \leftrightarrows S\lambda$ or $S\delta \leftrightarrows R\lambda$ enantiomeric exchange. In the $S\lambda/R\delta$ enantiomeric exchange process indicated in Scheme 4, the proton labeled as H(1) of the diastereotopic protons of the methylene group moves from environment B to A, and simultaneously, the proton labeled H(2) exchanges from environment A to B. This change of environments is the origin of the broadening of the signals.

The positive values obtained for $\Delta H^{\ddagger}$ (see Table 2) indicate that the overall process accounting for the dynamic behavior is endothermic. The negative values obtained for $\Delta S^{\ddagger}$ suggest an associative mechanism through a pentacoordinate intermediate with the participation of the solvent, [$PdCl_2$(κ^2-N∼N′)(DMSO)], similar to a result reported earlier.[20] In a second step, the partial decoordination of the ligand through the anilinic nitrogen to form [$PdCl_2$(κ^1-N∼N′)(DMSO)] allows the inversion of the configuration of that nitrogen atom, and its recoordination yields the *R*/*S* interconversion. The higher activation entropy found in **1d** compared with **1a** seems to be related to the electronic effect of the substituents on the aryl group. The electron withdrawing group makes the nitrogen atom less strongly coordinating, and the metal will be less rich in electronic density. This effect also makes the approach of a solvent molecule to form a pentacoordinate intermediate easier which, after breaking the Pd−N bond, will generate the tetracoordinate complex [$PdCl_2$(κ^1-N∼N′)(DMSO)].

Complexes of platinum with substituents on the *para* position of the aryl group (i.e., **2a**, **2c**, or **2d**) display a different behavior in solution of DMSO-d_6 when compared with their palladium analogues (**1a**, **1c**, or **1d**). These solutions evolve in a short period of time at room temperature to show new signals in the ^{1}H NMR spectrum, in addition to the signals of the starting complex. After a longer period of time, it is possible to see signals belonging to the free ligand, which suggests its complete decoordination. The early signals can be attributed to complexes with the ligand partially coordinated to the platinum atom. The coordinating solvent, DMSO, can occupy the vacant coordination positions of the metallic center.[21] For these processes, the softness of the DMSO sulfur atom seems to be the reason for the displacement of the pyridine-amine ligand (Scheme 5).

As found for palladium complex **1b**, the platinum complex with two methyl groups in positions 2 and 6 on the aryl ring

(16) Casares, J. A.; Espinet, P.; Soulantica, K.; Pascual, I.; Orpen, A. G. *Inorg. Chem.* **1997**, *36*, 5251−5256.
(17) Kapteijn, G. M.; Spee, M. P. R.; Grove, D. M.; Kooijman, H.; Spek, A. L.; van Koten, G. *Organometallics* **1996**, *15*, 1405−1413.
(18) Schulz, V.; Frick, A.; Huttner, G. *Eur. J. Inorg. Chem.* **2002**, 3111−3128.
(19) Frick, A.; Schulz, V.; Huttner, G. *Eur. J. Inorg. Chem.* **2002**, 3129−3147.
(20) Arnaiz, A.; Cuevas, J. V.; Garcia-Herbosa, G.; Carbayo, A.; Casares, J. A.; Gutierrez-Puebla, E. *J. Chem. Soc., Dalton Trans.* **2002**, 2581−2586.
(21) Dorta, R.; Rozenberg, H.; Shimon, L. J. W.; Milstein, D. *Chem.—Eur. J.* **2003**, *9*, 5237−5249.

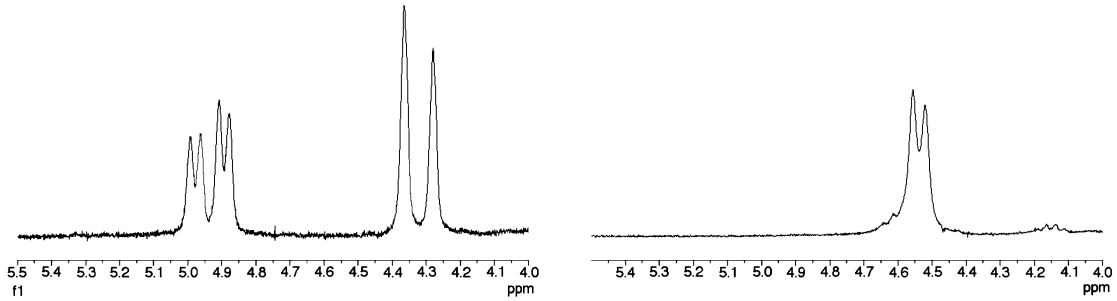

Figure 2. Comparison of ^{1}H NMR spectra in the methylene region (H^A and H^B) in complexes **1a** (left) and **1b** (right).

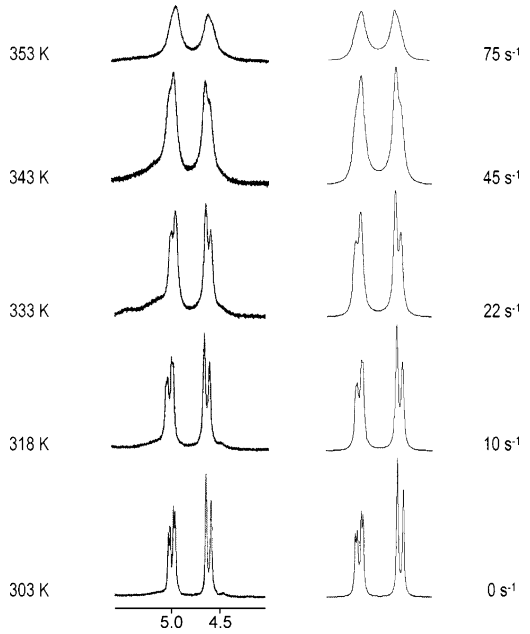

Figure 3. Methylene region of the ^{1}H NMR spectra of complex **1d** in the temperature range from 303 to 353 K and their simulations at the corresponding exchange rate.

Scheme 3

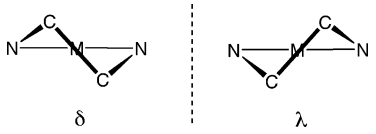

Scheme 4. Equilibrium $S\delta \leftrightarrows R\lambda$

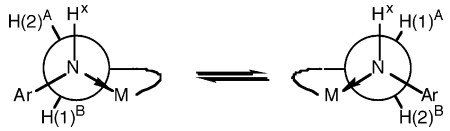

Table 2. Activation Parameters Calculated for the Enantiomeric Exchange Processes of **1a** and **1d**

compd	$\Delta H^{\ddagger}$/kJ·mol^{-1}	$\Delta S^{\ddagger}$/J·mol^{-1}	$\Delta G^{\ddagger\,a}$/kJ·mol^{-1}
1a	32(4)	−146(12)	78(8)
1d	52(3)	−64(9)	72(7)

[a] Estimated at 318 K.

of the ligand (**2b**) show a different behavior in solution. When a solution of this complex in DMSO-d_6 is heated, a separation of the chemical shifts of the protons is observed. The larger separation between signals when temperature is raised is responsible for a clearer presentation of the AB part of the ABX spin system (see Figure 4).

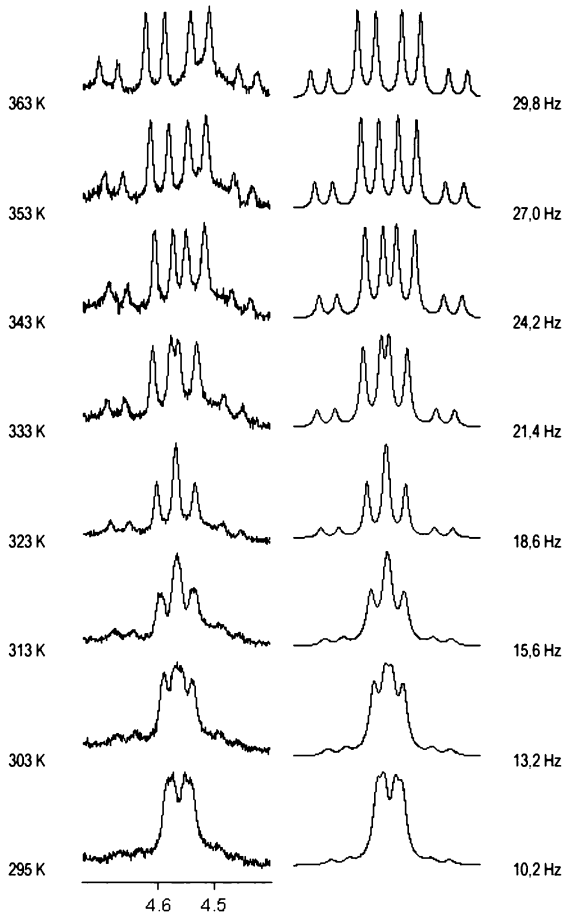

Figure 4. Methylene region of the ^{1}H NMR spectra of complex **2b** in the temperature range from 295 to 363 K and their simulations varying the gap (in Hz) between signals for H^A and H^B. (Complex **1b** showed a parallel behavior.)

Scheme 5

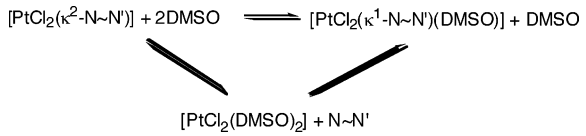

This behavior is observed for both palladium (**1b**) and platinum (**2b**) complexes. At first glance, it is surprising that a ligand with a bigger steric hindrance can be strongly coordinated to the metal. An explanation of this result might be found in the greater difficulty of approach for a molecule of DMSO to the metallic center with a bigger steric hindrance. In this way, the proposed pentacoordinate intermediate[20] cannot be formed, and the process of partial decoordination of the pyridine-amine ligand is not allowed.

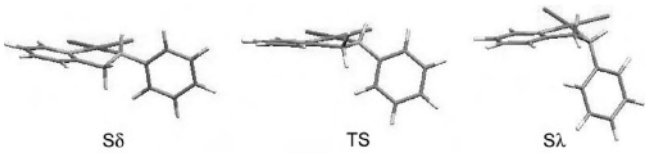

Figure 5. Calculated minima for the molecular structures of **1a**, and its transition state. Atomic coordinates are available in Supporting Information.

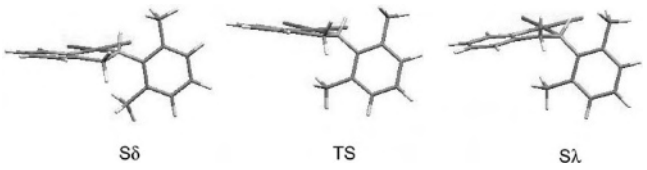

Figure 6. Molecular geometries, two minima and transition state, for optimized structures of **1b**. Atomic coordinates are available in Supporting Information.

Although there is not exchange $R-S$, the exchange $\delta \leftrightarrows \lambda$ is still going on because of the low barrier of this process (see below), and these spectra correspond to a mixture of diastereomers as we will discuss later.

Theoretical Calculations. In order to understand the behavior observed in solution, DFT quantum chemical calculations were carried out (see Experimental Section). For a model of complex **1a** in having an *S*-configuration for the anilinic nitrogen atom, and with the methyl in the *para* position removed, the λ conformation is 12.1 kJ·mol^{-1} more stable than the δ conformation. The λ to δ transition barrier is 15.4 kJ·mol^{-1}. Therefore, the most stable isomer of the couple $S\delta/S\lambda$ is $S\lambda$. In the same way, for the couple $R\delta/R\lambda$ the most stable isomer is $R\delta$, the enantiomer of $S\lambda$. Considering the calculated difference of energy between the isomers $S\lambda$ and $S\delta$, the statistical distribution of the population at 300 K is 0.76% for the δ isomer and 99.24% for the λ isomer, when the configuration of the anilinic nitrogen atom is *S*. Although the calculations were performed without considering the influence of the solvent in solution, we can state that the ^{1}H NMR spectrum corresponds to the enantiomers $S\lambda/R\delta$ because of the large calculated difference of populations. In the optimized structure for the model of complex **1a** (see Figure 5), the values of the torsion angles between the C−H bonds of the methylene of the chelating ring and the N−H (H^X) bond are 28.55° (for the torsion angle $H^A-C-N-H^X$) and −88.92° (for the torsion angle $H^B-C-N-H^X$). Cremer et al. have correlated the vicinal spin−spin coupling constants between protons belonging to five-membered rings with the torsion angle[22,23] giving a more specific example of the well-known correlation of Karplus.[24] The values of the coupling constants using this correlation are 8 and 0.5 Hz, respectively, which are not too far from the experimentally obtained 6.2 and ∼0 Hz (see Table 1) values. Despite the structure being optimized, isolated (without interactions of the solvent), and the system used for the correlation having some differences with our system (some of the atoms of the five membered ring are different), the values obtained are in good agreement with the ones experimentally determined in the ^{1}H NMR spectrum. The optimized structure is in good agreement with the NOE effects reported above: the atom labeled as H^B shows short distances to the hydrogen atoms in positions 2 and 6 of the 1,4-disubstituted phenyl ring and to the hydrogen atom in position 3 of the pyridine ring, and the atom labeled as H^A displays short distances to the aminic hydrogen, H^X, which is in good agreement with the observed NOEs.

An analogous quantum chemical calculation was carried out for complex **1b**. The results of this calculation indicate that with an *S*-configuration for the anilinic nitrogen atom, the conformation λ is 0.5 kJ·mol^{-1} more stable than the δ conformation. The barrier of the transition λ to δ is 1.1 kJ·mol^{-1}. As found for complex **1a**, the $S\lambda-R\delta$ enantiomers are more stable than the $R\lambda-S\delta$ enantiomers, but the difference of energy between these states is smaller for **1b** (see Figure 6). A calculation of the statistical distribution of the diastereomers at 300 K gives a distribution of populations of 54.6% for the more stable pair of enantiomers and 45.4% for the less stable pair. The small calculated energy barrier and the similarity of the populations thus generates a ^{1}H NMR dynamic spectrum with a contribution from both diastereomers. In the $S\lambda-R\delta$ isomers the values of the torsion angles between the C−H bonds of the methylene of the chelating ring and the N−H (H^X) bond are 3.55° and −112.37°, and with the correlation of Cremer et al.[22,23] the coupling constants between methylenic protons and H^X should be 9.5 and 3.0 Hz, respectively. In the isomers $R\lambda-S\delta$ the values of the torsion angles H−C−N−H are 44.45° and 160.27°, which gives theoretical values of the coupling constants between methylenic protons and H^X of 5.5 and 11.5 Hz, respectively. Because of the low energetic barrier for interconversion and the similarity of the values of the populations of both species, the actual values of the coupling constants should be an average of the theoretical values, which gives a result of 7.7 and 6.8 Hz, respectively. The experimental coupling constants for these spin systems at ambient temperature in complex **1b** are 6.8 and 8.0 Hz. A NOESY experiment displays proximity between one of these two protons and an *ortho*-methyl group. The proximity of the chemical shifts of both hydrogen atoms makes it difficult to distinguish which methylenic proton is close to that methyl group. Nevertheless, experimental and theoretical values of the coupling constants are very close. The observed differences probably arise from the differences between the theoretical model used in DFT calculations and the five-membered ring used for Cremer's correlation.[22,23]

Crystal Structures. The crystal structure of complex **2a** contains a racemic mixture of $S\lambda/R\delta$ enantiomeric pairs. The molecular structure of the $R\delta$ isomer is shown in Figure 7, and selected bond lengths, bond angles, and torsion angles are given in Table 3. The chelating ligand binds to the metal through a pyridyl donor N1 and secondary amine donor N2. The N1−Pt1−N2 bond angle is 83.13(13)°. The pyridyl donor makes a slightly shorter bond to the metal than does

(22) Wu, A. N.; Cremer, D.; Auer, A. A.; Gauss, J. *J. Phys. Chem. A* **2002**, *106*, 657−667.
(23) Wu, A.; Cremer, D. *J. Phys. Chem. A* **2003**, *107*, 1797−1810.
(24) Friebolin, H. *Basic One- and Two-Dimensional NMR Spectroscopy*, 3rd ed.; Wiley-VCH: Weinheim, Germany, 1998.

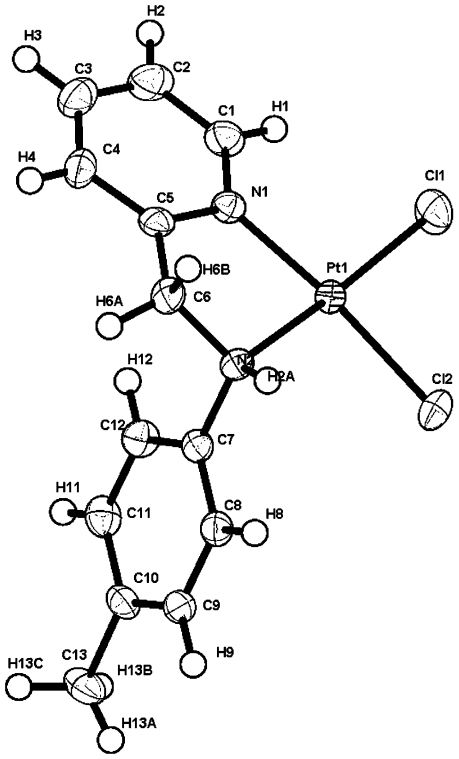

Figure 7. Molecular geometry for complex **2a**.

Table 3. Selected Bond Lengths (Å), Bond Angles (deg), and Torsion Angles (deg) for Complex **2a**

Pt1−N1	2.019(3)	Pt1−N2	2.059(3)
Pt1−Cl1	2.2952(12)	Pt1−Cl2	2.3047(11)
N1−Pt1−N2	83.13(13)		
N1−C5−C6−N2	−25.8(5)	H2A−C6−N2−H6A	−98.02
H2A−C6−N2−H6B	20.03		

the amine. The torsion angle N1−C5−C6−N2, −25.8(5)°, confirms that the isomer shown in Figure 7 is the *Rδ* isomer (as noted above, the *Sλ* isomer is also present in the crystal). This is in agreement with the theoretical calculations carried out for **1a**, that indicate that this enantiomeric pair gives the more stable diastereomers. The anisotropy of NOE interactions between the proton H2A and methylene protons H6A and H6B is evident in the solid-state torsion angles: H2A−N2−C6−H6A = −98° and H2A−N2−C6−H6B = 20°. The positions of the methylene hydrogen atoms involved are idealized according to the position and geometry of their parent atom, and thus, the torsion angle values should be interpreted with caution, but it is noteworthy that the values are not so far from the ones theoretically determined for complex **1a** and they display a good agreement with the correlation of Cremer et al.[22,23] Slight differences are expected to arise due to packing forces in the solid state.

X-ray quality crystals were also grown for **1b**. All of the comments made above concerning the solid-state structure of complex **2a** also apply for this complex. The molecular structure is shown in Figure 8, and selected bond distances, bond angles, and torsion angles are given in Table 4. The structure contains a racemic mixture of S*λ* and R*δ* enantiomers, as found for **2a**. The bond angles subtended by the chelating ligand at the metal in this complex are identical within experimental error to that found for complex **2a**. For

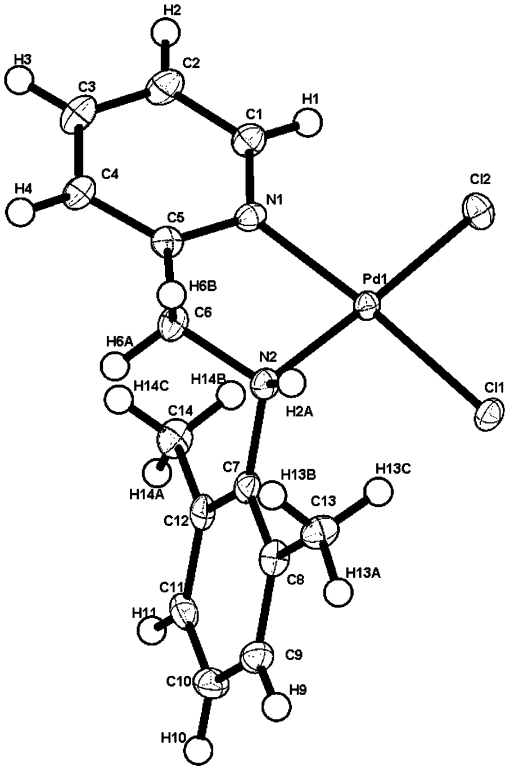

Figure 8. Molecular structure for complex **1b**.

Table 4. Selected Bond Lengths (Å), Bond Angles (deg), and Torsional Angles (deg) for Complex **1b**

Pd1−N1	2.032(3)	Pd1−N2	2.063(3)
Pd1−Cl1	2.2898(8)	Pd1−Cl2	2.3046(9)
N1−Pd1−N2	83.42(11)		
N1−C5−C6−N2	−17.0(4)	H2A−C6−N2−H6A	−113
H2A−C6−N2−H6B	4		

1b, the pyridyl N-donor atom of the chelating ligand makes a shorter bond to the metal than does the secondary amine N-donor. The torsion angle found for the atoms N1−C5−C6−N2 is −17.0(4)° confirming that the isomers shown in Figure 8 is the *Rδ* diastereomer in accord with the theoretical calculations. The torsion angles found for the H−C (methylenic) and N−H bonds are 4° and −113°, respectively. The positions of the methylene hydrogen atoms involved are idealized according to the position and geometry of their parent atom, and thus, these torsion angles should be interpreted with some caution, but as for complex **2a** these angles are close to those obtained for the more stable theoretical configuration.

Conclusions

Complexes of palladium with pyridine-amine ligands with little sterical hindrance display a dynamic behavior in solution, which has been assigned to an enantiomeric exchange *Sλ* ⇆ *Rδ* on the basis of dynamic ^{1}H NMR and quantum chemical calculations. This behavior is different from that observed for analogous platinum complexes in which equilibria of decoordination of the ligand are found (and substitution for molecules of the solvent). In all cases, a pentacoordinate intermediate can be proposed. For complexes containing ligands with a larger sterical hindrance (**1b**

and **2b**), no enantiomeric exchange has been observed. This fact can be understood by considering the more difficult formation of the pentacoordinate intermediate: the greater sterical hindrance makes the approach of a molecule of DMSO to the metallic center more difficult. In this way, the proposed pentacoordinate intermediate cannot be formed, and the process of partial decoordination of the pyridine-amine ligand is not allowed.

Experimental Section

General. Solvents were dried prior to use and stored under nitrogen. 2-Pyridine-carboxaldehide, *p*-toluensulfonic acid, 4-methylaniline, 2,6-dimethylaniline, 4-methoxyaniline, 4-trifluoromethylaniline, $PdCl_2$, LiCl, benzonitrile, Pt, $PtCl_2$, and $NaBH_4$ were commercial grade and were used without further purification. $[PtCl_2(NCPh)_2]$[25] and $K_2[PtCl_4]$[26] were synthesized according to published methods.

Characterization. Elemental analyses (C, H, N) were performed with a LECO CHNS-932 apparatus. Infrared spectra were recorded with a Nicolet Impact 410 FT-IR spectrophotometer in the 4000−400 cm^{-1} range, as KBr disks. ^1H and ^{13}C NMR spectra were obtained on a VARIAN UNITY INOVA spectrometer operating at 400 and 100 MHz, respectively, and using $SiMe_4$ as internal standard at 20 °C, and a VARIAN MERCURY 200 MHz spectrometer using $SiMe_4$ as internal standard at 20 °C. Mass analyses were performed on Micromass AutoSpec equipment.

Synthesis. The ligands were synthesized following a two-step procedure. The first step is the synthesis of an imine which is reduced to the amine on a second step.

$C_{13}H_{14}N_2$ (a). Step 1: Synthesis of the Imine $C_{13}H_{12}N_2$. A round bottomed flask was charged with 4-methylaniline (4.367 g, 40.76 mmol), 2-pyridine-carboxaldehyde (4.366 g, 40.76 mmol), a catalytic amount of *p*-toluensulfonic acid, and toluene (50 mL). The flask was equipped with a Dean−Stark condenser. The mixture was heated at reflux for 1 h, and then, the solvent was removed under vacuum yielding the imine as a oily residue. The imine was purified and recrystallized in hot hexanes affording a yellow solid. Yield: 6.226 g (78%). ^1H NMR (400 MHz, $CDCl_3$): 8.62 (ddd,^3J(H,H) = 4.8 Hz, ^4J(H,H) = 1.7 Hz, ^5J(H,H) = 0.9 Hz, 1H; H^6), 8.57 (s, 1H; CH═N); 8.11 (ddd,^3J(H,H) = 7.9 Hz, ^4J(H,H) = 1.0 Hz,^5J(H,H) = 0.9 Hz, 1H; H^3); 7.66 (ddd,^3J(H,H) = 7.9 Hz,^3J(H,H) = 7.5 Hz, ^4J(H,H) = 1.7 Hz, 1H; H^4); 7.22 (ddd,^3J(H,H) = 7.5 Hz, ^3J(H,H) = 4.8 Hz, ^4J(H,H) = 1.0 Hz, 1H; H^3); 7.17 (m, 2 H, 2 H^{aryl}); 7.14 (m, 2 H, 2 H^{aryl}); 2.29 (s, 3 H, CH_3). $^{13}C\{^1H\}$ NMR (100 MHz, $CDCl_3$): 159.81 (CH═N); 154.89 (C^2); 149.83 (C^6); 148.51 ($C^{ips°}$); 136.90 (C^4); 136.75; 130.05; 125.13 (C^{para}); 121.96; 121.34; 21.28 (CH_3). IR (KBr): $\tilde{\nu}$ (cm^{-1}) = 1627 (C═N); 822 and 767 (arC−H). MS *m*/*z* (%): 195 (100) [a^+ − H], 91 (77) [4-CH_3−$C_6H_4^+$], 79(63) [$C_5H_5N^+$]. Anal. Calcd (Found) for $C_{13}H_{12}N_2$: C, 79.56 (79.74); H, 6.16 (6.08); N, 14.27 (14.59).

Step 2: Synthesis of the Amine $C_{13}H_{14}N_2$ (a). A solution in methanol (60 mL) of the imine (4.6 g, 23.44 mmol) prepared in the first step was placed in a two-necked round bottomed flask equipped with a condenser. The solution was warmed to 50 °C. Slowly, $NaBH_4$ (1.5 g, 39.65 mmol) was added to the mixture with stirring. When the addition of $NaBH_4$ was complete, the mixture was heated at reflux for 30 min. After cooling, water (60 mL) was added to the yellow solution, and the mixture was concentrated under vacuum until the volume of solvent was reduced to one-quarter of its original volume. The product was extracted with diethyether (3 × 25 mL). All organic extracts were combined and dried over anhydrous magnesium sulfate. After filtering, the solvent was removed under vacuum yielding the amine as an orange solid. Yield 3.851 g (83%). ^1H NMR (200 MHz, $CDCl_3$): 8.56 (dd,^3J(H,H) = 4.9 Hz, ^4J(H,H) = 1.8 Hz, 1H; H^6); 7.59 (ddd,^3J(H,H) = 7.8 Hz, ^3J(H,H) = 7.5 Hz,^4J(H,H) = 1.8 Hz, 1 H; H^4); 7.31 (d,^3J(H,H) = 7.8 Hz, 1 H; H^3); 7.14 dd,^3J(H,H) = 7.5 Hz,^3J(H,H) = 4.9 Hz, 1 H; H^3); 6.97 (m, 2 H, 2 H^{aryl}); 6.58 (m, 2 H, 2 H^{aryl}); 4.42 (s, 2H; CH_2); 2.22 (s, 3 H, CH_3). $^{13}C\{^1H\}$ NMR (50 MHz, $CDCl_3$): 159.09 (C^2); 149.42 (C^6); 145.88; 136.85 (C^4); 129.99 (2 C^{meta}); 126.97; 122.27 (C^3); 121.82 (C^5); 113.42 (2 C^{ortho}); 49.90 (CH_2); 20.66 (CH_3). IR (KBr): $\tilde{\nu}$ (cm^{-1}) = 3308 (N−H); 803 and 760 (arC−H). MS *m*/*z* (%): 198 (43) [a^+], 120 (100) [a^+ − C_5H_4N]. Anal. Calcd (Found) for $C_{13}H_{14}N_2$: C, 78.75 (77.93); H, 7.12 (7.28); N, 14.13 (14.09).

$C_{14}H_{16}N_2$ (b). Step 1: Synthesis of the Imine $C_{14}H_{14}N_2$. The same procedure described for **a** is used with the following quantities: 2,6-dimethylaniline (4.610 g, 38.04 mmol), 2-pyridine-carboxaldehyde (4.075 g, 38.04 mmol). Yield: 6.226 g (78%). ^1H NMR (400 MHz, $CDCl_3$): 8.69 (ddd,^3J(H,H) = 4.8 Hz, ^4J(H,H) = 1.7 Hz, ^5J(H,H) = 0.9 Hz, 1H; H^6), 8.36 (s, 1 H; CH═N); 8.28 (ddd,^3J(H,H) = 7.9 Hz, ^4J(H,H) = 1.3 Hz, ^5J(H,H) = 0.9 Hz, 1 H; H^3); 7.78 (ddd,^3J(H,H) = 7.9 Hz, ^3J(H,H) = 7.5 Hz, ^4J(H,H) = 1.7 Hz, 1 H; H^4); 7.34 (ddd,^3J(H,H) = 7.5 Hz, ^3J(H,H) = 4.8 Hz, ^4J(H,H) = 1.3 Hz, 1H; H^3); 7.07 (m, 2 H, 2 H^{meta}); 6.67 (m, 1 H, H^{para}); 2.17 (s, 6 H, 2 CH_3). $^{13}C\{^1H\}$ NMR (100 MHz, $CDCl_3$): 163.72 (CH═N); 154.64 (C^2); 150.57 (C^{ipso}); 149.87 (C^6); 136.91 (C^4); 128.38 (2 C^{meta}); 127.05 (2 C^{ortho}); 125.57 (C^5); 124.32 (C^{para}); 121.44 (C^3); 18.57 (2 CH_3). IR (KBr): $\tilde{\nu}$ (cm^{-1}) = 1638 (C═N); 822, 776 (broad, arC−H). MS *m*/*z* (%): 209 (97) [a^+ − H], 195 (100) [a^+ − CH_3], 132 (51) [a^+ − C_5H_3N], 79 (62) [$C_5H_5N^+$]. Anal. Calcd (Found) for $C_{13}H_{14}N_2$: C, 79.97 (79.88); H, 6.71 (6.87); N, 13.32 (13.46).

Step 2: Synthesis of the Amine $C_{14}H_{16}N_2$ (b). The same procedure described for **a** is used with the following quantities: imine prepared in the first step (4.000 g, 19.02 mmol), $NaBH_4$ (1.500 g, 39.65 mmol). Yield: 3.736 g (93%) of a brown liquid. ^1H NMR (400 MHz, $CDCl_3$): 8.61 (ddd,^3J(H,H) = 4.9 Hz, ^4J(H,H) = 1.8 Hz, ^5J(H,H) = 0.9 Hz, 1 H; H^6); 7.63 (ddd,^3J(H,H) = 7.9 Hz, ^3J(H,H) = 7.5 Hz, ^4J(H,H) = 1.8 Hz, 1 H; H^4); 7.25 (ddd,^3J(H,H) = 7.9 Hz, ^3J(H,H) = 7.5 Hz, ^4J(H,H) = 1.2 Hz, ^5J(H,H) = 0.9 Hz, 1 H; H^3); 7.19 (ddd,^3J(H,H) = 7.5 Hz, ^3J(H,H) = 4.9 Hz, ^4J(H,H) = 1.2 Hz, 1 H; H^5); 7.00 (m, 2 H, 2 H^{meta}); 6.83 (m, 1 H, H^{para}); 4.29 (s, 2 H; CH_2); 4.27 (s broad, 1 H; NH); 2.33 (s, 6 H, 2 CH_3). $^{13}C\{^1H\}$ NMR (100 MHz, $CDCl_3$): 159.33 (C^2); 149.48 (C^6); 146.34 (C^{ipso}); 136.65 (C^4); 129.71 (2 C^{ortho}); 122.32 (2 C^{meta}); 122.32 (C^5); 122.20 (C^3); 122.06 (C^{para}); 53.86 (CH_2); 18.89 (2 CH_3). IR (polyethylene): $\tilde{\nu}$ (cm^{-1}) = 3356 (N−H); 760 (broad, arC−H). MS *m*/*z* (%): 212 (20) [a^+], 120 (100) [$(CH_3)_2$−C_6H_3−NH^+], 93 (76) [C_5H_4N−CH_3^+], 80 (47) [$C_5H_6N^+$]. Anal. Calcd (Found) for $C_{14}H_{16}N_2$: C, 79.21 (78.86); H, 7.60 (7.88); N, 13.20 (13.18).

$C_{13}H_{14}N_2O$ (c). Step 1: Synthesis of the Imine $C_{13}H_{12}N_2O$. The same procedure described for **a** is used with the following quantities: 4-methoxyaniline (6.158 g, 50.00 mmol), 2-pyridine-carboxaldehyde (5.356 g, 50.00 mmol). Yield: 6.226 g (78%) of a brown solid. ^1H NMR (400 MHz, $CDCl_3$): 8.70 (ddd, ^3J(H,H) = 4.8 Hz, ^4J(H,H) = 1.7 Hz, ^5J(H,H) = 0.9 Hz, 1 H; H^6), 8.63 (s, 1 H; CH═N); 8.18 (ddd, ^3J(H,H) = 7.9 Hz, ^4J(H,H) = 1.2 Hz, ^5J(H,H) = 0.9 Hz, 1 H; H^3); 7.80 (ddd, ^3J(H,H) = 7.9 Hz, ^3J(H,H) = 7.5 Hz, ^4J(H,H) = 1.7 Hz, 1 H; H^4); 7.34 (m partially overlapped

(25) Braunstein, P.; Bender, R.; Jud, J.; Vahrenkamp, H.; Vogel, G. C.; Geoffroy, G. L. *Inorg. Synth.* **1989**, *26*, 341−350.
(26) Kauffman, G. B. *Inorg. Synth.* **1963**, *7*, 220−224.

to the H^{ortho} signal of the anysyl ring, $^3J(H,H) = 7.5$ Hz, $^4J(H,H) = 1.7$ Hz, 1H; H^5); 7.34 (m, 2 H, 2 H^{meta}); 6.95 (m, 2 H, 2 H^{para}); 3.84 (s, 3 H, OCH_3). $^{13}C\{^1H\}$ NMR (100 MHz, $CDCl_3$): 159.13 (C^{para}); 158.45 (CH═N); 155.05 (C^2); 149.86 (C^6); 143.87 (C^{ipso}); 136.83 (C^4); 125.04 (2 C^5); 122.89 (2 C^{ortho}); 121.87 (C^3); 114.65 (C^{meta}); 55.70 (OCH_3). IR (KBr): $\tilde{\nu}$ (cm^{-1}) = 1626 (C═N); 830, 777 (broad, arC−H). MS *m*/*z* (%): 212 (93) [a^+], 211 (79) [$a^+ - H$], 79 (100) [$C_5H_5N^+$]. Anal. Calcd (Found) for $C_{13}H_{12}N_2O$: C, 73.56 (73.10); H, 5.70 (5.60); N, 13.20 (13.25).

Step 2. Synthesis of the Amine $C_{13}H_{14}N_2O$ (c). The same procedure described for **a** is used with the following quantities: imine prepared in the first step (6.452 g, 30.40 mmol), $NaBH_4$ (1.702 g, 45.00 mmol). Yield: 3.736 g (93%) of a white solid. ^1H NMR (400 MHz, $CDCl_3$): 8.58 (ddd, $^3J(H,H) = 4.9$ Hz, $^4J(H,H) = 1.8$ Hz, $^5J(H,H) = 0.9$ Hz, 1 H; H^6); 7.63 (ddd, $^3J(H,H) = 7.9$ Hz, $^3J(H,H) = 7.5$ Hz, $^4J(H,H) = 1.8$ Hz, 1 H; H^4); 7.33 (d broad, $^3J(H,H) = 7.9$ Hz, 1 H; H^3); 7.17 (ddd, $^3J(H,H) = 7.5$ Hz, $^3J(H,H) = 4.9$ Hz, $^4J(H,H) = 1.2$ Hz, 1 H; H^5); 6.78 (m, 2 H, 2 H^{meta}); 6.63 (m, 2 H, 2 H^{ortho}); 4.41 (s, 2 H; CH_2); 4.38 (s broad, 1 H; NH); 3.73 (s, 3 H, OCH_3). $^{13}C\{^1H\}$ NMR (100 MHz, $CDCl_3$): 159.03 (C^2); 152.40 (C^{para}); 149.44 (C^6); 142.36 (C^{ipso}); 136.82 (C^4); 122.27 (C^5); 121.87 (C^3); 115.06 (C^{meta}); 114.50 (C^{ortho}); 55.98 (OCH_3); 50.47 (CH_2). IR (KBr): $\tilde{\nu}$ (cm^{-1}) = 3281 (N−H); 821, 782 (broad, arC−H). MS *m*/*z* (%): 214 (60) [a^+], 136 (71) $a^+ - C_5H_4N$], 92 (100) [$C_5H_4N-CH_2^+$]. Anal. Calcd (Found) for $C_{13}H_{14}N_2O$: C, 72.87 (72.40); H, 6.59 (6.44); N, 13.07 (13.15).

$C_{13}H_{11}F_3N_2$ (d). Step 1: Synthesis of the Imine $C_{13}H_9F_3N_2$. The same procedure described for **a** is used with the following quantities: 4-trifluoromethylaniline (3.500 g, 21.72 mmol), 2-pyridine-carboxaldehyde (2.326 g, 21.72 mmol). Yield: 6.226 g (78%) of a white solid. ^1H NMR (400 MHz, $CDCl_3$): 8.74 (ddd, $^3J(H,H) = 4.8$ Hz, $^4J(H,H) = 1.7$ Hz, $^5J(H,H) = 0.9$ Hz, 1 H; H^6), 8.57 (s, 1 H; CH═N); 8.21 (ddd, $^3J(H,H) = 7.9$ Hz, $^4J(H,H) = 1.2$ Hz, $^5J(H,H) = 0.9$ Hz, 1 H; H^3); 7.85 (ddd, $^3J(H,H) = 7.9$ Hz, $^3J(H,H) = 7.6$ Hz, $^4J(H,H) = 1.7$ Hz, 1 H; H^4); 7.68 (m, 2 H, 2H^{meta}); 7.42 (ddd, $^3J(H,H) = 7.6$ Hz, $^3J(H,H) = 4.8$ Hz, $^4J(H,H) = 1.2$ Hz, 1 H; H^5); 7.33 (m, 2 H, 2 H^{ortho}). $^{13}C\{^1H\}$ NMR (100 MHz, $CDCl_3$): 162.69 (CH═N);1 54.37 (C^{ipso}); 150.10 (C^6); 137.05 (C^4); 128.59 (q, $^2J(C,F) = 32.5$ Hz, 1 C, C^{para}); 126.68 (q, $^3J(C,F) = 3.6$ Hz, 2 C, C^{meta}); 125.86 (C^5); 124.40 (q, $^1J(C,F) = 272.3$ Hz, 1 C, CF_3); 122.45 (C^3); 121.34 (2 C^{ortho}). IR (KBr): $\tilde{\nu}$ (cm^{-1}) = 1622 (C═N); 841, 782 (broad, arC−H). MS *m*/*z* (%): 249 (100) [$a^+ - H$], 145 (59) [$CF_3-C_6H_4^+$], 79 (75) [$C_5H_5N^+$]. Anal. Calcd (Found) for $C_{13}H_9F_3N_2$: C, 62.40 (58.56); H, 3.63 (4.28); N, 11.20 (10.61).

Step 2. Synthesis of the Amine $C_{13}H_{11}F_3N_2$ (d). The same procedure described for **a** is used with the following quantities: imine prepared in the first step (3.000 g, 11.99 mmol), $NaBH_4$ (0.680 g, 17.97 mmol). Yield: 2.499 g (83%) of a white solid. ^1H NMR (400 MHz, $CDCl_3$): 8.58 (d, $^3J(H,H) = 4.7$ Hz, 1 H; H^6); 7.66 (ddd, $^3J(H,H) = 7.7$ Hz, $^3J(H,H) = 7.5$ Hz, $^4J(H,H) = 1.4$ Hz, 1 H; H^4); 7.40 (m, 2 H, 2 H^{meta}); 7.29 (d broad, $^3J(H,H) = 7.8$ Hz, 1 H; H^3); 7.20 (m, H^5); 6.67 (m, 2 H, 2 H^{ortho}); 5.28 (s broad, 1 H; NH); 4.47 (d, $^3J(H,H) = 5.1$ Hz, 2 H; CH_2). $^{13}C\{^1H\}$ NMR (100 MHz, $CDCl_3$): 157.13; 150.22; 149.20; 136.72; 126.55; 123.60; 122.33; 121.55; 118.70; 112.09; 48.44. IR (KBr): $\tilde{\nu}$ (cm^{-1}) = 3367 (N−H); 829, 760 (broad, arC−H). Anal. Calcd (Found) for $C_{13}H_{11}F_3N_2$: C, 61.90 (61.71); H, 4.40 (4.43); N, 11.11 (11.13).

Complexes of palladium (**1a**−**d**) were prepared following the general procedure described for **1a**.

[$PdCl_2$(a)] (1a). A solution of $Li_2[PdCl_4]$ was prepared by slowly heating a mixture of $PdCl_2$ (0.231 g, 1.30 mmol) and LiCl (0.110 g, 2.60 mmol) in methanol (45 mL). A methanolic solution of amine **a** (0.259 g, 1.30 mmol) was slowly added over the filtered solution of $Li_2[PdCl_4]$ with stirring. The orange precipitate formed was collected on a fritted glass funnel and washed with cold methanol and diethyl ether. Yield: 0.320 g (66%). ^1H NMR (400 MHz, DMSO-d_6): 8.73 (d, $^3J(H,H) = 5.8$ Hz, 1 H; H^6); 8.71 (d, $^3J(H,H) = 6.2$ Hz, 1 H; N−H); 8.15 (dd, $^3J(H,H) = 7.8$ Hz, $^3J(H,H) = 7.7$ Hz, 1 H; H^4); 7.76 (d, $^3J(H,H) = 7.8$ Hz, 1 H; H^3); 7.58 (dd, $^3J(H,H) = 7.7$ Hz, $^3J(H,H) = 5.8$ Hz, 1 H; H^5); 7.09 (m, 2 H, H^{meta}); 6.98 (m, 2 H, 2 H^{ortho}); 4.93 (dd, $^2J(H,H) = 16.9$ Hz, $^3J(H,H) = 6.2$ Hz, 1 H; CH^AH^B H near to NH); 4.32 (d, $^2J(H,H) = 16.9$ Hz, 1 H; CH^AH^B H near to aryl ring); 2.21 (s, 3 H, CH_3). IR (KBr): $\tilde{\nu}$ (cm^{-1}) = 3200 (N−H); 814 and 765 (arC−H). Anal. Calcd (Found) for $C_{13}H_{14}N_2Cl_2Pd$: C, 41.57 (41.10); H, 3.76 (3.38); N, 7.46 (7.78).

[$PdCl_2$(b)] (1b). The same procedure is used as that for **1a** with the following quantities: $PdCl_2$ (0.231 g, 1.300 mmol), LiCl (0.110 g, 2.600 mmol), and **b** (0.276 g, 1.300 mmol). Yield: 0.409 g (81%) of an orange solid. ^1H NMR (400 MHz, DMSO-d_6): 8.90 (d, $^3J(H,H) = 5.7$ Hz, 1 H; H^6); 8.09 (dd, $^3J(H,H) = 7.7$ Hz, $^3J(H,H) = 7.4$ Hz, 1 H; H^4); 7.82 (dd, $^3J(H,H) = 8.0$ Hz, $^3J(H,H) = 6.8$ Hz, 1 H; N−H); 7.55 (dd, $^3J(H,H) = 7.4$ Hz, $^3J(H,H) = 5.7$ Hz, 1 H; H^5); 7.54 (d, $^3J(H,H) = 7.7$ Hz, 1 H; H^3); 7.10 (m, 1 H, H^{meta}); 7.05 (m, 1 H, H^{para}); 6.98 (m, 1 H, H^{meta}); 4.54 (dd, $^2J(H,H) = 18.0$ Hz, $^3J(H,H) = 6.8$ Hz, 1 H; CH^AH^B); 4.51 (dd, $^2J(H,H) = 18.0$ Hz, $^3J(H,H) = 8.0$ Hz, 1 H; CH^AH^B); 3.12 (s, 3 H, CH_3), 2.32 (s, 3 H, CH_3). IR (KBr): $\tilde{\nu}$ (cm^{-1}) = 3220 (N−H); 781 and 760 (arC−H). Anal. Calcd (Found) for $C_{14}H_{16}N_2Cl_2Pd$: C, 43.16 (43.10); H, 4.14 (4.18); N, 7.19 (7.08).

[$PdCl_2$(c)] (1c). The same procedure is used as that for **1a** with the following quantities: $PdCl_2$ (0.231 g, 1.300 mmol), LiCl (0.110 g, 2.600 mmol), and **c** (0.279 g, 1.300 mmol). Yield: 0.458 g (90%) of an orange solid. ^1H NMR (200 MHz, DMSO-d_6): 8.72 (d, $^3J(H,H) = 5.7$ Hz, 1 H; H^6); 8.66 (d broad, 1 H; N−H); 8.13 (dd, $^3J(H,H) = 7.8$ Hz, $^3J(H,H) = 7.7$ Hz, 1 H; H^4); 7.73 (d, $^3J(H,H) = 7.7$ Hz, 1 H; H^3); 7.56 (dd, $^3J(H,H) = 7.8$ Hz, $^3J(H,H) = 5.7$ Hz, 1 H; H^5); 7.02 (m, 2 H, H^{aryl}); 6.84 (m, 2 H, 2 H^{aryl}); 4.90 (dd, $^2J(H,H) = 16.8$ Hz, $^3J(H,H) = 5.4$ Hz, 1 H; CH^AH^B H near to NH); 4.30 (d, $^2J(H,H) = 16.9$ Hz^3, 1 H; CH^AH^B H near to aryl ring); 3.67 (s, 3 H, OCH_3). IR (KBr): $\tilde{\nu}$ (cm^{-1}) = 3197 (N−H); 828 and 775 (arC−H). Anal. Calcd (Found) for $C_{13}H_{14}N_2Cl_2OPd$: C, 39.87 (39.40); H, 3.60 (3.69); N, 7.15 (7.37).

[$PdCl_2$(d)] (1d). The same procedure is used as that for **1a** with the following quantities: $PdCl_2$ (0.231 g, 1.300 mmol), LiCl (0.110 g, 2.600 mmol), and **d** (0.328 g, 1.300 mmol). Yield: 0.475 g (85%) of an orange solid. ^1H NMR (200 MHz, DMSO-d_6): 9.13 (s broad, 1 H; N−H); 8.74 (d, $^3J(H,H) = 5.6$ Hz, 1 H; H^6); 8.18 (dd, $^3J(H,H) = 7.9$ Hz, $^3J(H,H) = 7.8$ Hz, 1 H; H^4); 7.77 (d, $^3J(H,H) = 7.9$ Hz, 1 H; H^3); 7.60 (dd, $^3J(H,H) = 7.8$ Hz, $^3J(H,H) = 5.6$ Hz, 1 H; H^5); 7.70 (m, 2 H, H^{aryl}); 7.30 (m, 2 H, 2 H^{aryl}); 4.97 (dd, $^2J(H,H) = 16.8$ Hz, $^3J(H,H) = 5.4$ Hz, 1 H; CH^AH^B H near to NH); 4.57 (d, $^2J(H,H) = 16.8$ Hz, 1 H; CH^AH^B H near to aryl ring). IR (KBr): $\tilde{\nu}$ (cm^{-1}) = 3185 (N−H); 838 and 766 (arC−H). Anal. Calcd (Found) for $C_{13}H_{11}N_2Cl_2F_3Pd$: C, 36.35 (36.35); H, 2.58 (2.16); N, 6.52 (6.83).

[$PtCl_2$(a)] (2a). A solution of $K_2[PtCl_4]$ (1.047 g, 2.520 mmol) in water (25 mL) was placed in a round bottom flask. Amine **a** (0.500 g, 2.52 mmol) was dissolved in water acidified with concentrated HCl, and this solution was added to the first solution. The mixture was heated at reflux for 6 h, and a yellow precipitate was obtained. This solid was collected on a fritted glass funnel and washed with cold methanol and diethyl ether. Yield: 0.989 g (85%). ^1H NMR (400 MHz, DMSO-d_6): 9.25 (d, $^3J(H,H) = 5.9$ Hz, 1 H; N−H); 9.06 (d, $^3J(H,H) = 5.7$ Hz, 1 H; H^6); 8.22 (dd, $^3J(H,H) = 7.8$ Hz, $^3J(H,H) = 7.8$ Hz, 1 H; H^4); 7.76 (d, $^3J(H,H) = 7.8$ Hz, 1 H; H^3); 7.56 (dd, $^3J(H,H) = 7.8$ Hz, $^3J(H,H) = 5.7$ Hz,

1 H; H^5); 7.09 (m, 2 H, H^{meta}); 6.98 (m, 2 H, 2 H^{ortho}); 4.75 (dd, ^2J(H,H) = 16.9 Hz, ^3J(H,H) = 6.2 Hz, 1 H; CH^AH^B H near to NH); 4.41 (d, ^2J(H,H) = 16.9 Hz, 1 H; CH$^AH^B$ H near to aryl ring); 2.22 (s, 3 H, CH_3). IR (KBr): $\tilde{\nu}$ (cm^{-1}) = 3148 (N−H); 834 and 817 (arC−H). Anal. Calcd (Found) for $C_{13}H_{14}N_2Cl_2Pt$: C, 33.63 (33.76); H, 3.04 (2.97); N, 6.03 (6.00).

[PtCl$_2$(b)] (2b). A solution of [$PtCl_2(NCPh)_2$] (0.472 g, 1.000 mmol) in THF (50 mL) was placed in a round bottom flask. The mixture is warmed to 70 °C for some minutes to help dissolution. Amine **b** (0.212 g, 1.000 mmol) was dissolved in THF, and this solution was added to the first one. The mixture was heated at reflux for 14 h, and a yellow precipitate was obtained. This solid was collected on a fritted glass funnel and washed with cold methanol and diethyl ether. Yield: 0.375 g (78%). ^{1}H NMR (400 MHz, DMSO-d_6): 9.22 (d, ^3J(H,H) = 5.9 Hz, 1 H; H^6); 8.17 (dd, ^3J(H,H) = 8.0 Hz, ^3J(H,H) = 7.8 Hz, 1 H; H^4); 8.10 (dd, ^3J(H,H) = 7.1 Hz, ^3J(H,H) = 7.1 Hz, 1 H; N−H); 7.57 (d, ^3J(H,H) = 8.0 Hz, 1 H; H^3); 7.09 (dd, ^3J(H,H) = 7.8 Hz, ^3J(H,H) = 5.9 Hz, 1 H; H^5); 7.09 (m, 1 H, H^{meta}); 7.06 (m, 1 H, H^{para}); 7.01 (m, 1 H, H^{meta}); 4.59 (dd, ^2J(H,H) = 17.7 Hz, ^3J(H,H) = 7.1 Hz, 1 H; CH^AH^B); 4.54 (dd, ^2J(H,H) = 17.7 Hz, ^3J(H,H) = 7.1 Hz, 1 H; CH$^AH^B$ H); 3.02 (s, 3 H, CH_3), 2.37 (s, 3 H, CH_3). IR (KBr): $\tilde{\nu}$ (cm^{-1}) = 3222 (N−H); 787 and 768 (arC−H). Anal. Calcd (Found) for $C_{14}H_{16}N_2Cl_2Pt$: C, 35.16 (35.06); H, 3.37 (3.14); N, 5.86 (5.80).

[PtCl$_2$(c)] (2c). A solution of [$PtCl_2(NCPh)_2$] (0.165 g, 0.350 mmol) in THF (20 mL) was placed in a round bottom flask. The mixture was warmed to 70 °C for some minutes to help the dissolution. Amine **c** (0.075 g, 0.350 mmol) was dissolved in THF, and this solution was added to the previous one. The mixture was heated at reflux for 7 h, and a yellow precipitate was obtained. This solid was collected on a fritted glass funnel and washed with cold methanol and diethyl ether. Yield: 0.110 g (66%). ^{1}H NMR (200 MHz, DMSO-d_6): 9.23 (d broad, 1 H; N−H); 9.07 (d, ^3J(H,H) = 5.9 Hz, 1 H; H^6); 8.22 (dd, ^3J(H,H) = 7.9 Hz, ^3J(H,H) = 7.7 Hz, 1 H; H^4); 7.76 (d, ^3J(H,H) = 7.9 Hz, 1 H; H^3); 7.56 (dd, ^3J(H,H) = 7.7 Hz, ^3J(H,H) = 5.9 Hz, 1 H; H^5); 7.05 (m, 2 H, H^{aryl}); 6.87 (m, 2 H, 2 H^{aryl}); 4.74 (dd, ^2J(H,H) = 16.7 Hz, ^3J(H,H) = 6.1 Hz, 1 H; CH^AH^B H near to NH); 4.41 (d, ^2J(H,H) = 16.7 Hz,^{3} 1 H; CH$^AH^B$ H near to aryl ring); 3.70 (s, 3 H, OCH_3). IR (KBr): $\tilde{\nu}$ (cm^{-1}) = 3097 (N−H); 828 and 775 (arC−H). Anal. Calcd (Found) for $C_{13}H_{14}N_2Cl_2OPt$: C, 32.51 (34.85); H, 2.94 (3.40); N, 5.83 (5.75).

[PtCl$_2$(d)] (2d).: A solution of $K_2[PtCl_4]$ (0.330 g, 0.790 mmol) in water (20 mL) was placed in a round bottom flask. Amine **d** (0.200 g, 0.79 mmol) was dissolved in water acidified with concentrated HCl, and this solution was added to the first one. The mixture was heated at reflux for 4 h, and a yellow precipitate was obtained. This solid was collected on a fritted glass funnel and washed with cold methanol and diethyl ether. Yield: 0.202 g (49%). ^{1}H NMR (200 MHz, DMSO-d_6): 9.70 (s broad, 1 H; N−H); 9.06 (d, ^3J(H,H) = 5.8 Hz, 1 H; H^6); 8.25 (dd, ^3J(H,H) = 7.8 Hz, ^3J(H,H) = 7.8 Hz, 1 H; H^4); 7.78 (d, ^3J(H,H) = 7.8 Hz, 1 H; H^3); 7.72 (m, 2 H, H^{aryl}); 7.59 (dd, ^3J(H,H) = 7.8 Hz, ^3J(H,H) = 5.6 Hz, 1 H; H^5); 7.29 (m, 2 H, 2 H^{aryl}); 4.84 (dd, ^2J(H,H) = 16.9 Hz, ^3J(H,H) = 6.1 Hz, 1 H; CH^AH^B H near to NH); 4.63 (d, ^2J(H,H) = 16.9 Hz, 1 H; CH$^AH^B$ H near to aryl ring). IR (KBr): $\tilde{\nu}$ (cm^{-1}) = 3122 (N−H); 776 and 764 (arC−H). Anal. Calcd (Found) for $C_{13}H_{11}N_2Cl_2F_3Pt$: C, 30.13 (31.62); H, 2.14 (2.25); N, 5.41 (5.71).

X-ray Structure Determination. Crystallographic data for compounds **1b** and **2a** were collected at 173K on Bruker-AXS SMART[27] 1k diffractometers at the School of Chemistry, University of Bristol using Mo Kα radiation (λ = 0.71073 Å). Intensity data were collected as a series of frames, each of ω width 0.3°, integrated[28] and corrected for absorption[29] and solved and refined using routine techniques.[30] The amine hydrogen atom, H2A in each complex, was located in the electron density difference map and refined without positional restraints. Methyl hydrogen atoms positions were assigned by rotating group refinement with fixed C−H distances and H−C−H angles. All other hydrogen atoms were assigned idealized positions in accord with the position and geometry of their parent atom. All non-hydrogen atoms were refined with anisotropic diaplacement parameters. The isotropic displacement parameters for hydrogen atoms H2A in each complex were allowed to refine freely. All other hydrogen atoms were assigned isotropic displacement parameters equal to 1.5 times (methyl hydrogen atoms) or 1.2 times (all other hydrogen atoms) that of their parent atom. Key crystallographic data are given in Table 5.

Table 5. Crystallographic Data

	1b	**2a**
formula	$C_{14}H_{16}Cl_2N_2Pd$	$C_{13}H_{14}Cl_2N_2Pt$
M	389.59	464.25
cryst syst	monoclinic	orthorhombic
cell dimensions	a = 10.1689(11) Å	a = 9.978(2) Å
	b = 12.880(2) Å	b = 14.061(3) Å
	c = 11.736(2) Å	c = 20.115(6) Å
	β = 109.516(12)°	
unit cell volume/Å^3	1448.7(4)	2822.1(12)
space group	$P2_1/n$	$Pbca$
Z	4	8
μ/mm^{-1}	1.636	10.305
reflns measured/unique/obsd[a]	16428/3326/2767	17026/3224/2614
R_{int}	5.3%	4.2%
R1[b]	3.2%	2.3%
wR2[c]	7.5%	5.6%

[a] Observation criterion: $I > 2\sigma(I)$. [b] Calculated for observed data. [c] Calculated for all unique data.

Computational Study. Initial optimizations of the models were carried out at the semiempirical level PM3[31] implemented on MacSpartan 1.0.3 package.[32] DFT calculations were performed with the hybrid method known as B3LYP, in which the Becke three-parameter exchange functional[33] and the Lee−Yang−Parr correlation functional were used,[34] implemented in the Gaussian 98 (Revision A.09) program suite.[35] Relativistic effective core potentials from Stuttgart-Dresden group were used to represent the innermost electrons of the palladium atom and its basis set of

(27) *SMART diffractometer control software*; Bruker Analytical X-ray Instruments Inc.: Madison, WI, 1998.
(28) *SAINT integration software*; Bruker-AXS Inc.: Madison, WI, 2004.
(29) Sheldrick, G. M. *SADABS: A program for absorption correction with the siemens SMART system*; University of Göttingen: Göttingen, Germany, 2003.
(30) *SHELXTL program system*, version 5.1; Bruker Analytical X-ray Instruments Inc.: Madison, WI, 2003.
(31) Stewart, J. J. P. *J. Comput. Chem.* **1989**, *10*, 209−220.
(32) Wavefunction, I.; 1.0.2 ed.: Irvine, CA, 1999−2000.
(33) Becke, A. D. *J. Chem. Phys.* **1993**, *98*, 5648−5652.
(34) Lee, C. T.; Yang, W. T.; Parr, R. G. *Phys. Rev. B* **1988**, *37*, 785−789.
(35) Frisch, M. J.; Trucks, G. W.; Schlegel, H. B.; Scuseria, G. E.; Robb, M. A.; Cheeseman, J. R.; Zakrzewski, V. G.; Montgomery, J. A., Jr.; Stratmann, R. E.; Burant, J. C.; Dapprich, S.; Millam, J. M.; Daniels, A. D.; Kudin, K. N.; Strain, M. C.; Farkas, O.; Tomasi, J.; Barone, V.; Cossi, M.; Cammi, R.; Mennucci, B.; Pomelli, C.; Adamo, C.; Clifford, S.; Ochterski, J.; Petersson, G. A.; Ayala, P. Y.; Cui, Q.; Morokuma, K.; Malick, D. K.; Rabuck, A. D.; Raghavachari, K.; Foresman, J. B.; Cioslowski, J.; Ortiz, J. V.; Stefanov, B. B.; Liu, G.; Liashenko, A.; Piskorz, P.; Komaromi, I.; Gomperts, R.; Martin, R. L.; Fox, D. J.; Keith, T.; Al-Laham, M. A.; Peng, C. Y.; Nanayakkara, A.; Gonzalez, C.; Challacombe, M.; Gill, P. M. W.; Johnson, B. G.; Chen, W.; Wong, M. W.; Andres, J. L.; Head-Gordon, M.; Replogle, E. S.; Pople, J. A. *Gaussian 98*, revision A.09; Gaussian, Inc.: Pittsburgh, PA, 1998.

valence double-ζ quality associated known as SDD.[36] The basis set for the main group elements was split-valence and included polarization functions in all atoms (C, N, Cl, and H, abbreviated as SVP).[37] The geometries for the each minimum were fully optimized in all isomers, and transition states are confirmed by a vibrational analysis.

Acknowledgment. The authors gratefully acknowledge the European Commission (LIFE05 ENV/E/000333), the Spanish Ministerio de Educación y Ciencia (BQ2002-01039 and CTQ2005-03141), and the Junta de Castilla y León (BU14/03) for financial support. We also acknowledge the Servicios Centrales de Apoyo a la Investiación (SCAI) of the Universidad de Burgos for technical support.

(36) Andrae, D.; Haussermann, U.; Dolg, M.; Stoll, H.; Preuss, H. *Theor. Chim. Acta* **1990**, *77*, 123−141.
(37) Schafer, A.; Horn, H.; Ahlrichs, R. *J. Chem. Phys.* **1992**, *97*, 2571−2577.

Supporting Information Available: X-ray crystallographic files in CIF format and tables of atomic coordinates of optimized structures (Tables S1−S6). This material is available free of charge via the Internet at http://pubs.acs.org.

IC061060U